JGP Journal of General Physiology

VIEWPOINT

The muscle M3 x-ray diffraction peak and sarcomere length: No evidence for disordered myosin heads out of actin overlap

John M. Squire[1,2] and Carlo Knupp[3]

X-ray diffraction studies of muscle have provided a wealth of information on muscle structure and physiology, and the meridian of the diffraction pattern is particularly informative. Reconditi et al. (2014. *J. Physiol.* https://doi.org/10.1113/jphysiol.2013.267849) performed superb experiments on changes to the M3 meridional peak as a function of sarcomere length (SL). They found that the M3 intensity dropped almost linearly as sarcomere length increased at least to about SL = 3.0 µm, and that it followed the same track as tension, pointing toward zero at the end of overlap at ∼3.6 µm. They concluded that, just as tension could only be generated by overlapped myosin heads, so ordered myosin heads contributing to the M3 intensity could only occur in the overlap region of the A-band, and that nonoverlapped heads must be highly disordered. Here we show that this conclusion is not consistent with x-ray diffraction theory; it would not explain their observations. We discuss one possible reason for the change in M3 intensity with increasing sarcomere length in terms of increasing axial misalignment of the myosin filaments that at longer sarcomere lengths is limited by the elastic stretching of the M-band and titin.

Introduction

The axial part of the diffraction patterns from striated muscles, the meridian, provides a wealth of information about muscle structure, including the behavior of the myosin heads (see reviews in Squire, 1981; Harford and Squire, 1997; Squire, 2000; Squire and Knupp, 2005, 2017; Squire, 2019), but it is vital to consider what can genuinely be deduced from the diffraction data. Fig. 1 a shows intensity traces along the meridian from the seminal work of Haselgrove (1975). Diffraction peaks labeled M1 etc. are mainly from the myosin filament including C-protein. The peak labeled T1 is from the troponin–tropomyosin complex on the thin filaments. The peak at M3 with a spacing ∼145.7 Å for active muscle is the third order of the myosin axial repeat of ∼437 Å and corresponds roughly to the axial separation of successive crowns of myosin heads along the myosin filaments (Squire, 1972; Al-Khayat et al., 2013).

In Fig. 1 a, there are many very closely spaced peaks. These have been known for many years to be due to interference between the similar structures in the two halves of the A-band (Rome et al., 1973). Fig. 1 b, from Squire and Knupp (2017), based on an illustration in Squire (1981; page 581), shows how interference occurs and also that, if two populations of myosin heads have slightly different conformations, then the interference distance (L) between the two diffracting arrays would change, in this case from L1 to L2. Fig. 1 c shows how an underlying M3 peak from the myosin heads on one half of a myosin filament at ∼145.7 Å for active muscle may be sampled by closely spaced interference fringes so that the underlying peak is split, in this case into two components.

Reconditi et al. (2014) performed elegant experiments in which they studied the frog muscle diffraction pattern as a function of sarcomere length (SL). The bridge regions on each half of the A-band have stripes of the extra protein C-protein (myosin binding protein C; Offer et al., 1973; Squire, 1981; Bennett et al., 1986; Squire et al., 2003; Luther et al., 2011) in their central region, forming the C-zone (Sjöström and Squire, 1977; Fig. 1 d). With changing SL, the amount of overlap between the myosin and actin filaments gradually changes (Fig. 1 d) until at an SL of ∼3.0 µm, the C-zone is no longer overlapped by actin. Then, at SL = 3.6 µm, the actin filaments come completely out of overlap with the myosin filaments. Reconditi et al. (2014) monitored the intensity of the M3 peak during tetanus (the

[1]Muscle Contraction Group, School of Physiology, Pharmacology & Neuroscience, University of Bristol, Bristol, UK; [2]Faculty of Medicine, Imperial College London, London, UK; [3]School of Optometry and Vision Sciences, Cardiff University, Cardiff, UK.

John M. Squire died on January 31, 2021; Correspondence to Carlo Knupp: knuppc@cardiff.ac.uk

This work is part of a special collection on myofilament function and disease.

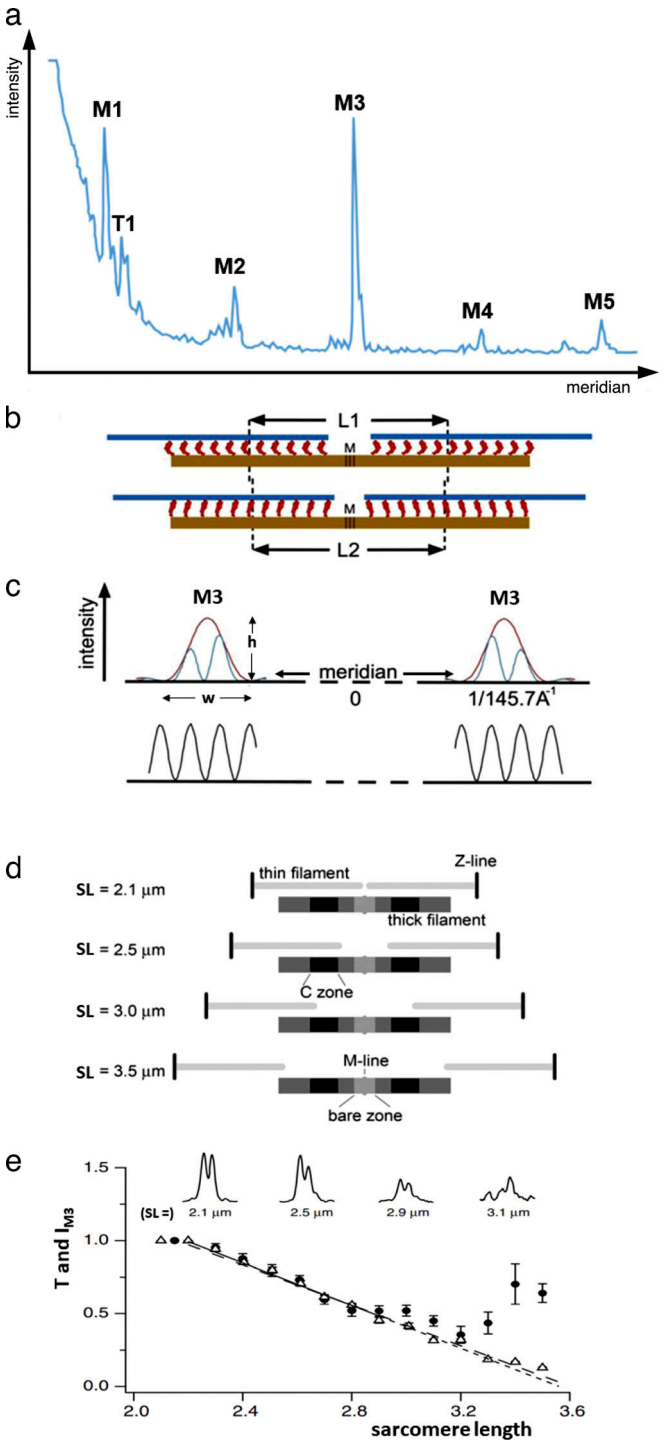

Figure 1. **Interference effects on meridional x-ray reflections. (a)** Intensity profile along the meridian from frog muscle in the relaxed state, from the work of Haselgrove (1975). Reflections from myosin are labeled M1, M2, etc. T1 comes from the troponin/tropomyosin complex. The fine sampling of the diffraction patterns comes from interference between the diffracted x-rays from the two halves of the A-band as in b and c. **(b)** Schematic representation of how the interference distance might change (from L1 to L2) if the myosin heads on actin change their configuration. **(c)** Schematic representation of how the underlying M3 peak from one half A-band (top) is sampled by the interference function with closely spaced peaks (bottom) to give, in this case, an M3 doublet. Note the M3 peak height (h) and peak width (w). **(a)** Adapted from Haselgrove (1975); b and c reproduced from Squire and Knupp (2017). **(d)** Variation of the overlap of the actin and myosin filaments as SL increases. Each half A-band has stripes of C-protein (myosin binding protein C) in the C-zone. At around SL = 3 µm, the C-zone is hardly overlapped by actin filaments. At SL = 3.6 µm, the actin and myosin overlap reduces to zero. **(e)** Observed variation of tension (triangles) and I_{M3} (filled circles) as the frog fiber SL is gradually increased. Both tension and M3 intensity reduce almost linearly as SL increases at least to ~3.0 µm. Inset shows the M3 profiles at different SLs. From 2.1 to 2.9 µm, the separation of the two interference peaks appears not to change. **(d and e)** Figure reproduced from Reconditi et al. (2014) with permission.

integrated weighted sum of the two interference peaks) as a function of SL as shown in Fig. 1 e. They found an almost linear reduction of M3 intensity up to an SL of ~3.0 µm, after which the signal became very noisy but tended to increase. The tension reduced in the same way as the M3 intensity on approximately the same line to about SL = 3.0 µm, but then continued to change linearly down to zero at SL = 3.6 µm. The insets to Fig. 1 e show the profiles of the M3 peak at different SLs.

Reconditi et al. (2014) interpreted their observations as meaning that, in active muscle, heads not overlapped by actin must be sufficiently disordered that they did not contribute to the observed M3 peak. In the same way that only overlapped heads can produce tension, they claimed that only overlapped heads could contribute to the M3 from active muscle. To quote: "The dispersion of the (nonoverlapped) heads is sufficiently large compared with their ca 14.5 nm axial repeat that they make almost no contribution to the M3 reflection." They also said, and the insets in Fig. 1 e appear to confirm this, that, to quote, there is "no change in the interference fine structure" with SL. But there is a fundamental error in this analysis by Reconditi et al. (2014); they missed several important points.

Modeling the suggestion of Reconditi et al.

Taking the conclusion of Reconditi et al. (2014) at its face value gives the results in Figs. 2, 3, and 4. In Fig. 2, a–c, as SL increases, the overlap region (lo) of the A-band becomes axially smaller (red boxes), and the box separation, the interference distance L, gradually increases. We show three different situations with interference length L_s (short SL), L_m (middle SL), and L_L (long SL). As SL increases, the axial extent (lo) of the overlap region reduces, so the M3 peak from one half of the overlapped A-band (i.e., in the red boxes) will gradually get weaker because there are fewer diffracting objects, and will gradually broaden axially because the axial extent of the red boxes is shorter (the width of the unsampled M3 peak is marked by w in Fig. 1 c; the unsampled peak comes only from one half of the sarcomere). Also, the interference distance L gradually increases, so the interference peaks crossing the M3 will gradually get closer together and will be narrower. At the same time, more interference peaks will sample the broadened underlying M3 peak.

Because L changes by multiples of the myosin periodicity, the interference function around the M3 peak is approximately the same (being exactly the same only at the frequency corresponding to the reciprocal of the myosin periodicity). All of these effects are very clear in Fig. 3 b.

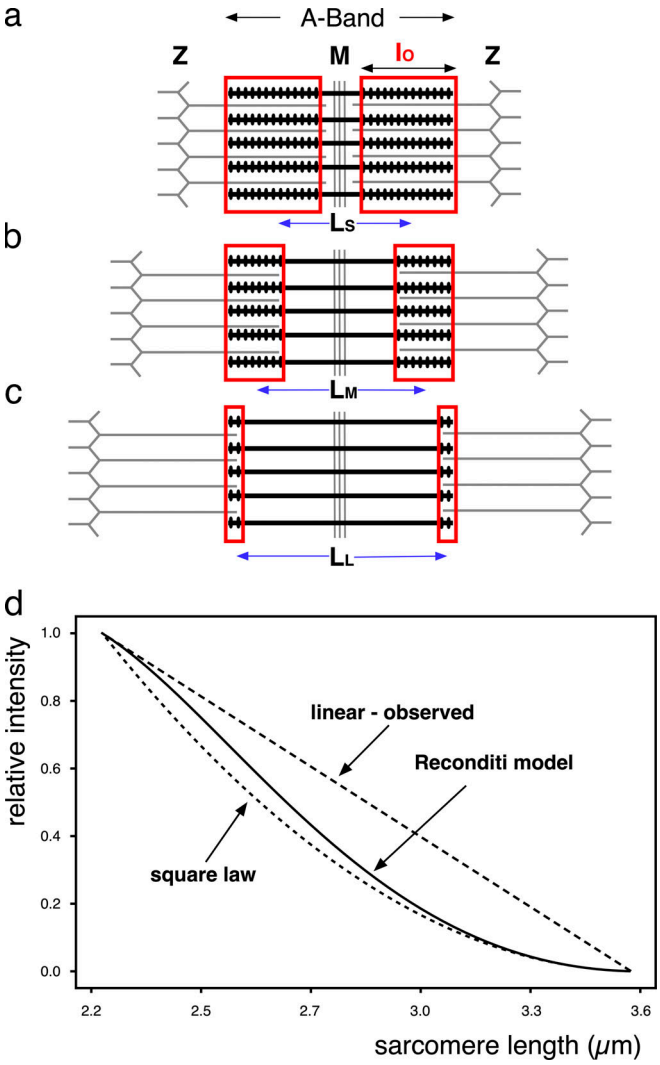

Figure 2. **Effects of sarcomere length changes. (a–c)** Illustration of the effect of SL change on the diffracting region as the overlap of the actin and myosin filaments gradually reduces. The red boxes show that the axial extent (length of overlap lo) of the diffracting object reduces and the interference length L increases as SL increases, in these case from L_s to L_m to L_L. **(d)** Plots of the predicted M3 intensity between SL = 2.2 µm and SL = 3.6 µm as observed (linear, dashed line out to 3.0 µm), as predicted if by a square law (dotted line), and as would be expected from the Reconditi et al. (2014) model with the two central M3 peaks getting closer together as the interference length L increases and the overlap length lo gradually reduces (see a–c and Fig. 3). For details, see text.

Another point is this. The integrated intensity of a diffraction peak from an array that is N objects long is determined by the peak height, which varies as the square of N, multiplied by the peak width, which is related to 1/N. Reconditi et al. (2014) say that the observed peak widths do not change with SL. If the peak width does not change, then the total intensity in the peaks would vary as the peak height, which is a function of N^2. So, even if only overlapped heads contributed to the M3, there should not be a linear change of M3 intensity with SL, but a change related to the square of the amount of overlap (Fig. 2 d, dotted line).

The situation is actually slightly more complicated than this. For short sarcomeres, we have that the interference function peak heights are proportional to the square of the overlap length (lo), but the two interference peaks almost fill the whole of the unsampled M3 peak, and its width (w in Fig. 1 c) is proportional to 1/lo. Therefore, the total integrated intensity (proportional to width times height; i.e., to $lo^2 \times 1/lo$) for small SLs does vary almost linearly with overlap. However, as SL increases, the unsampled M3 peak gets broader, and more and more interference peaks sample it (Fig. 4 a), so the two central interference peaks, which are also getting narrower, are sampling less and less of this underlying peak, and the intensity change of the sampled M3 peaks gradually transitions from linear to being proportional to the square of the amount of overlap. This trend is shown by the solid line in Fig. 2 d.

In conclusion, the idea of Reconditi et al. (2014) that non-overlapped heads do not contribute to the M3 from active muscle and that the M3 only comes from the overlapped heads does not work. This model would predict the presence of extra satellite peaks within the observed M3 profiles, as in Fig. 4 a, and not seen in the insets in Fig. 1 e, and the intensity of the central two interference peaks would vary as in Fig. 2 d, solid line, and not linearly, as observed. Since much of the further analysis in that paper rested on this basic untenable interpretation of their data, their further conclusions need to be reconsidered.

At the very least, to reproduce the experimental data, the detached/nonoverlapping heads must be contributing as much to the M3 at longer SLs as they do at full overlap.

We have discussed elsewhere some of the hazards of making deductions about myosin head behavior from one or two low-resolution meridional reflections (Knupp et al., 2009; see also Squire and Knupp, 2021).

Can a distribution of attached and detached myosin heads explain the observations?

In Knupp et al. (2009), the changes in the M3 peak as observed by the Irving and Lombardi group and their collaborators (Piazzesi et al., 2002; Huxley et al., 2006) involved in small muscle length changes were explained by the relative axial movement of two myosin head populations, one a detached population (70% of the total) and a second actin-attached population (30% of the total). Both populations were represented by 145.7 Å-spaced Gaussian densities, with the detached population Gaussian slightly narrower axially than the attached Gaussian. Relative axial movements of these two populations could explain a host of M3 intensity observations (see Knupp et al. [2009] for references and details). We wondered if this kind of model would explain the change of the M3 intensity with SL discussed above (Fig. 1 e). We considered the possibility that out of overlap, the majority of the myosin heads on each crown might mostly be in the "heads out" conformation of Hudson et al. (1997) (see Knupp et al., 2019, and Squire and Knupp, 2021) and that in overlap, the heads would be as in the model of Knupp et al. (2009) discussed above. However, we found that this would not explain the observations, and no other combination of head configurations that we tried worked well either. This does not mean that the M3 observations in Fig. 1 e are definitely not to do with some combination of different head conformations, it only means that, as yet, we have not found one that works. However, there is another kind of interpretation that might work.

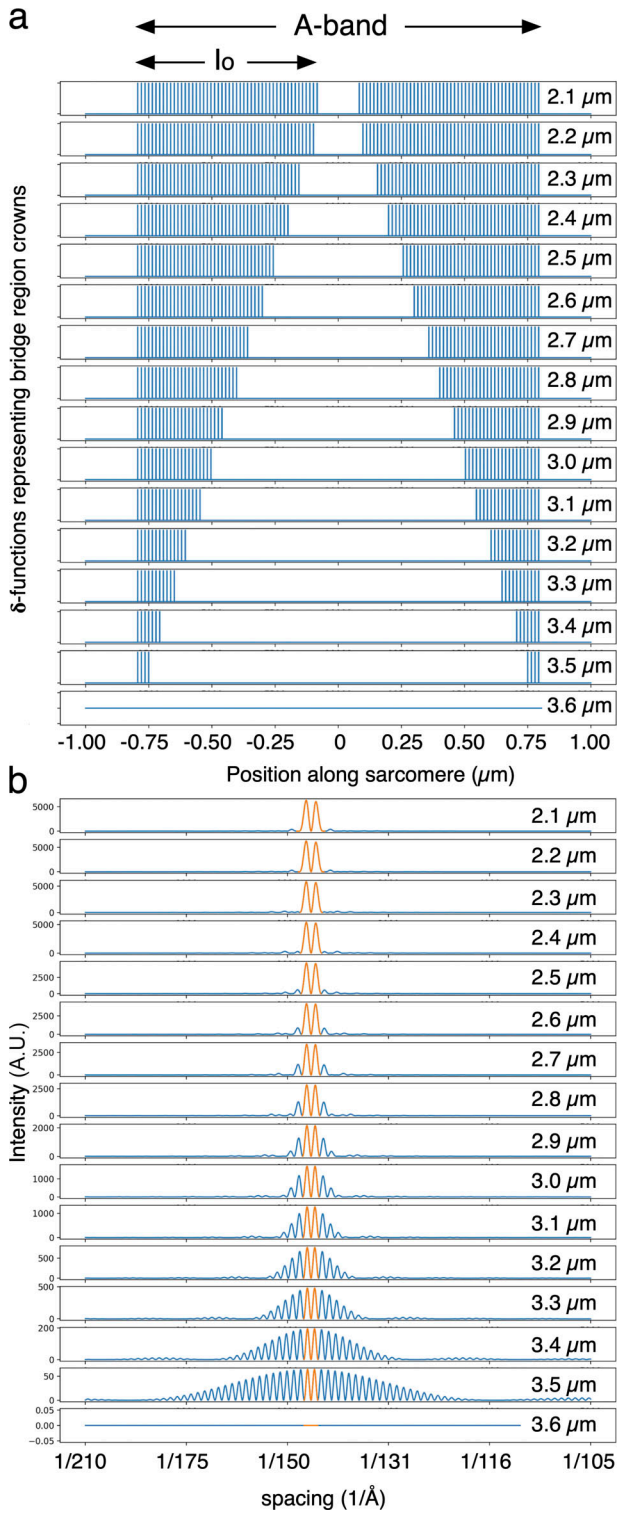

Figure 3. **Calculations showing the origin of the predicted M3 intensity change.** Related to Fig. 2 d. **(a)** 50 145.7 Å–spaced crowns of overlapped heads, represented as δ-functions, in each half A-band at full overlap (SL = 2.1 μm) at the top and down to SL = 3.6 μm at the bottom. **(b)** The computed diffraction pattern as SL changes. There are three things to note: (1) as SL increases the red boxes in Fig. 2, a–c gradually reduce in axial extent (lo), so the underlying M3 peak from one half of the A-band gradually becomes broader along the meridian, and gradually includes more and more interference peaks; (2) the central peaks gradually become weaker; the scales on the left of the figures gradually change from 5,000 arbitrary units (A.U.) at the top (2.2 μm) to 50 for the second-lowest trace (3.5 μm). The height of the unsampled M3 peak (h in Fig. 1 c) reduces as the square of the amount of filament overlap; and (3) the interference peaks gradually get closer together as SL increases. The integrated intensities of the central two peaks colored orange here give the solid line plot in Fig. 2 d. This plot is what would be expected from the model of Reconditi et al. (2014) if only cross-bridges overlapping the actin filaments contribute to the M3 peak, whereas their observations show a linear change in M3 as SL increases to ∼3.0 μm (Fig. 1 e). For details, see text.

A possible alternative interpretation

If it is not due to disordered heads, what could produce the observed, almost linear, drop of the M3 intensity with SL (Fig. 1 e) down to ∼3.0 μm followed by an increase? We know from the lack of change of the interference function (the inserts in Fig. 1 e show no changes in peak width) that at least to ∼3.0 μm, the M3 peak comes from the whole of the bridge region of the A-band since the interference distance has not changed. Second, the M3 peak must come from myosin heads or C-protein or part of the filament backbone, including the A-band part of titin. We do not know of anything else in the sarcomere that would contribute to the M3. Third, it is likely to come from the whole bridge region because the inset diffraction patterns in Fig. 1 e do not have additional satellite interference peaks to each side of the main two peaks as would occur (see Fig. 3 b) if the red box length (lo) in Fig. 2, a–c, was reducing, or was only part of the bridge region, giving axially broader underlying M3 profiles.

A possible explanation for the systematic reduction of the M3 in Fig. 1 e is that it is well-known that across the A-band, the axial register of the myosin filaments and actin filaments deteriorates as the SL increases (Huxley et al., 1982; Bordas et al., 1993; Martin-Fernandez et al., 1994). Eakins et al. (2019) calculated the sort of change one might see in M3 intensity as the axial disorder increased. The axial disorder was represented as random axial shifts of 100 myosin filaments within bounds described by the width σ_a of a Gaussian function along the fiber axis. The result, shown here as Fig. 4 b, was that the M3 intensity would decrease substantially with increased axial disorder and could be knocked down to zero if the axial disorder was large enough (approximately at σ = 45–50 Å). A drop of roughly 50%, which occurs in Fig. 1 e at an SL of ∼2.9 μm, would only require axial shifts within a Gaussian spread of width ∼20 Å, not an unreasonable value. The interference distance along the meridian would probably be largely unaffected by this axial disorder; the averaged crown mass projected onto the meridian would gradually increase in axial extent, but the interference distance would be exactly the same, and the interference peaks would remain sharp.

Why the drop in the M3 intensity should be almost exactly linear with SL (Fig. 1 c) is hard to assess, but one possibility from Fig. 4 b is that in full overlap muscle, there is already axial myosin filament disorder defined by a Gaussian spread of ∼10 Å axial width (point A in Fig. 4 b), and then, as the SL increases, the axial disorder increases steadily until at SL = 2.9 μm it reaches a Gaussian width of ∼20 Å (point B in Fig. 4 b), still quite a small number, where the intensity will have dropped to 50% of its starting value. The drop between the two values could be almost linear (Fig. 4 b). But why should the M3 intensity then

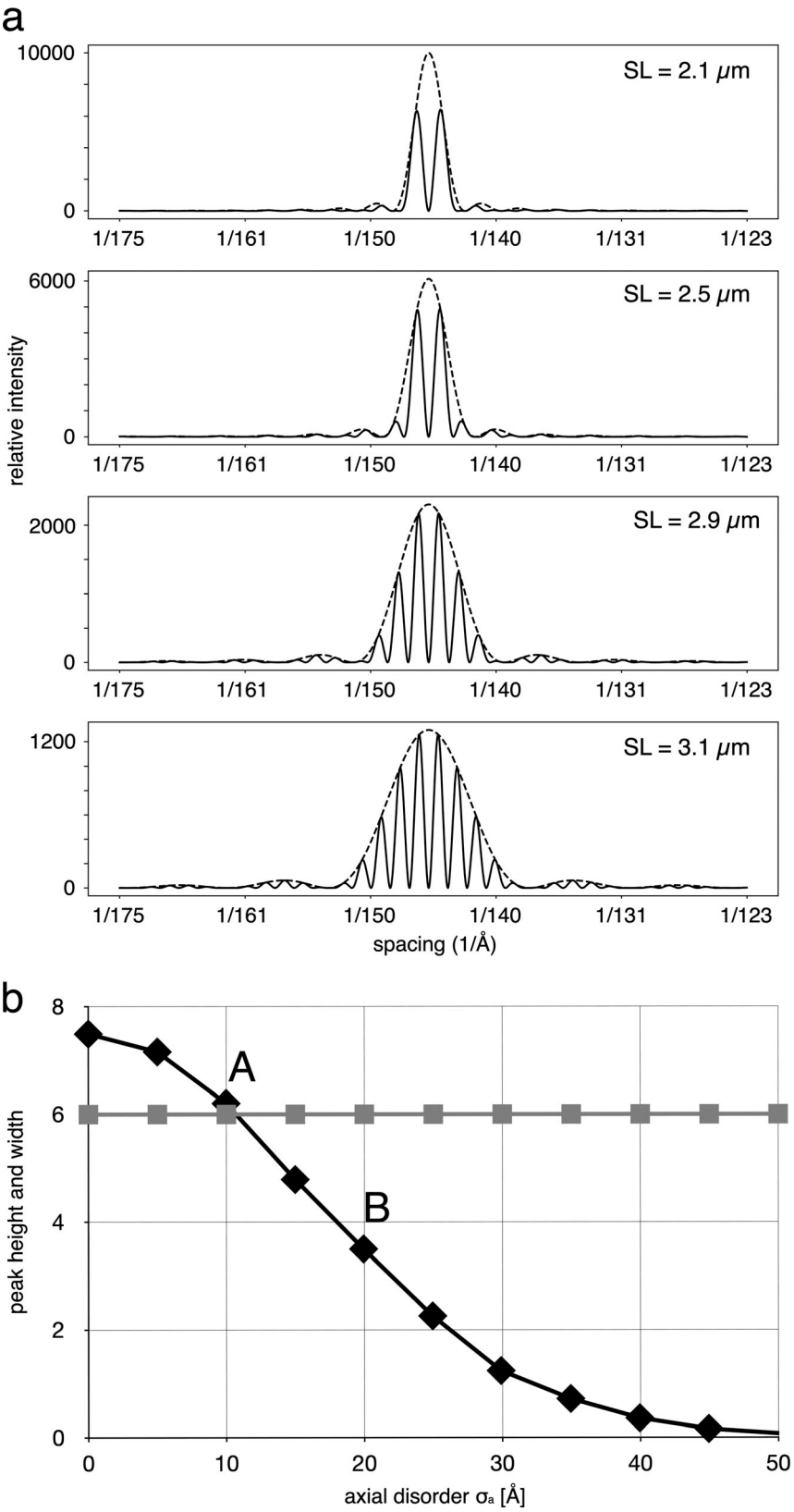

Figure 4. **Simulation of the expected M3 peak behavior. (a)** Selected calculated diffraction patterns from Fig. 3 b for the SLs shown in the insets of Fig. 1 e if the Reconditi et al. (2014) proposal is correct. Note that as SL increases, more and more peaks are sampling the underlying M3 peak. The appearance of the peaks is not at all like those in Fig. 1 e, where no satellite peaks are seen. **(b)** Plots of the calculated peak height (diamonds) and peak width (squares) across the meridian of the M3 meridional reflection as myosin filaments in the A-band are given ever increasing axial displacements within limits set by the axial disorder parameter σ_a, which represents the width of a Gaussian distribution along the fiber axis. If in active muscle the axial disorder was to increase from around σ_a = 10 Å at SL = 2.2 µm (point A) to around σ_a = 20 Å at SL = 2.9 µm (point B), then there might be an almost linear reduction in the M3 intensity with SL increase as observed by Reconditi et al. (2014). For an explanation of why the width of the M3 peaks remains constant, see Fig. 9 of Eakins et al. (2019). Figure adapted from Eakins et al. (2019).

stop reducing in the same way between SL = 2.8 and 3.2 µm and then start going up again as SL increases beyond ~3.2 µm (Fig. 1 e)? One possibility might be that the myosin filaments are cross-linked in the M-band by a complex assembly of myomesin, M-protein, and titin (Lange et al., 2020) which form an elastic constraint on the myosin filaments. Any axial disorder of the myosin filaments will be opposed by distortion of the M-band protein complex. Perhaps after a certain axial displacement, the

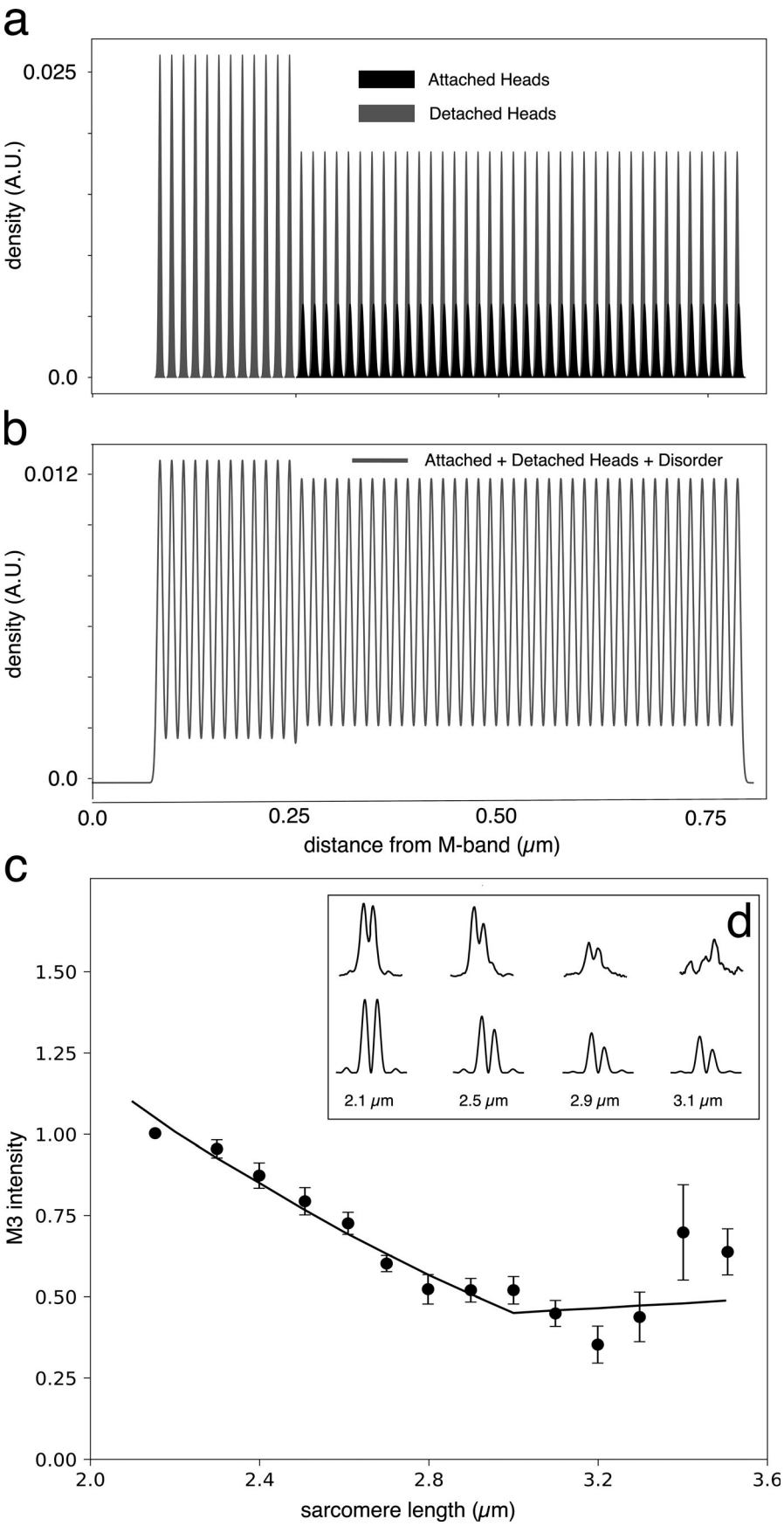

Figure 5. **New possible explanation. (a–c)** Model of a half A-band at an SL of 2.5 µm according to the results of Knupp et al. (2009) with the M-band on the left-hand edge. Cross-bridge densities in active frog muscle are represented throughout the calculations as Gaussian density profiles on each of 50 myosin head crown positions, 145 Å apart. In the overlap region, 30% of the myosin heads are actin-attached, and 70% of the heads are detached. The Gaussian profiles for the two states are slightly different, with the detached Gaussians slightly narrower than the attached Gaussians. There is also a small axial displacement between the two sets with the active heads ∼20 Å further from the M-band (see Knupp et al., 2009). In the nonoverlap region, 100% of the heads are in the detached configuration. In the new explanation for the M3 changes with SL, all these Gaussian densities were summed, and then further Gaussian smoothing was imposed to represent axial disorder of the whole myosin filament. The resulting density profile for SL = 2.5 µm is in b. The calculated M3 intensity from the models in a and b for different values of SL are shown in c, with the inclusion of a limit to the axial spread at ∼3.0 µm due to the combined effects of the M-band and titin. The black dots and error bars are from the results in Reconditi et al. (2014) as in Fig. 1 e. **(d)** Top row: The observed M3 profiles from Reconditi et al. (2014) as in Fig. 1 e. Bottom row: The same profiles according to the new model in a and b. The agreement between the profiles is quite good but starts to break down at 3.1 µm. A.U., arbitrary units.

M-band tends to stop the myosin filaments from having axial excursions that are too great. The effect of this would be to make the M3 intensity tend to stop changing for larger SLs. In addition to this, in many muscles, it is at SLs ∼3 µm that the tension due to titin extension starts to come into play (Brynnel et al., 2018). Titin provides the increase in resting tension in relaxed muscles as SL increases. Titin may also contribute to the reduction in myosin filament axial shifting at around SLs beyond ∼3 µm.

We have modeled this possibility starting with the results of Knupp et al. (2009), with the M3 intensity in active muscle due to 30% of the heads attached to actin and force-producing and 70% of the heads still detached. We then superimposed on this model at different SLs, various levels of axial disorder in the myosin filaments, and in the head-attachment sites on actin. An example of this model is shown in Fig. 5 a for an SL of 2.5 µm. In the nonoverlap part of the A-band, the detached-head Gaussians represent 100% of the heads. In the overlap region, the attached population is 30% and the detached population 70% of the total number of heads. If gradually increasing axial disorder is imposed as the SL increases, then the M3 intensity can drop almost linearly down to ∼3.0 µm (Fig. 5 c). If the M-band and titin then impose constraints on the axial displacement of the myosin filaments, but the SL continues to increase from 3.0 to 3.6 µm, the M3 intensity can start to go up again, as observed (Fig. 5 c). At the same time, the profiles of the two M3 subpeaks change in a manner very similar to the observations of Reconditi et al. (2014) as in Fig. 5 c, at least to ∼3.0 µm. So the effects of axial misalignment of the myosin filaments could explain the M3 intensity changes with SL, but there may be other explanations.

Conclusion

In conclusion, to be consistent with x-ray diffraction theory, the excellent observations of Reconditi et al. (2014) require a different explanation from the one they describe, and there is in fact no evidence in that paper that nonoverlapped heads are disordered and do not contribute to the M3 peak. However, it is possible that the observed active M3 changes with overlap are due to axial displacements of the myosin filaments and that at longer SLs, these displacements are limited by the elastic restoring forces in the M-band and titin.

Acknowledgments

Henk L. Granzier served as editor.

J.M. Squire was associated with the fellowship grant to Dr. Danielle Paul from the British Heart Foundation (#FS/14/18/3071).

The authors declare no competing financial interests.

Author contributions: J.M. Squire and C. Knupp carried out the analysis; J.M. Squire and C. Knupp wrote the paper.

References

AL-Khayat, H.A., R.W. Kensler, J.M. Squire, S.B. Marston, and E.P. Morris. 2013. Atomic model of the human cardiac muscle myosin filament. *Proc. Natl. Acad. Sci. USA.* 110:318–323. https://doi.org/10.1073/pnas.1212708110

Bennett, P., R. Craig, R. Starr, and G. Offer. 1986. The ultrastructural location of C-protein, X-protein and H-protein in rabbit muscle. *J. Muscle Res. Cell Motil.* 7:550–567. https://doi.org/10.1007/BF01753571

Bordas, J., G.P. Diakun, F.G. Diaz, J.E. Harries, R.A. Lewis, J. Lowy, G.R. Mant, M.L. Martin-Fernandez, and E. Towns-Andrews. 1993. Two-dimensional time-resolved X-ray diffraction studies of live isometrically contracting frog sartorius muscle. *J. Muscle Res. Cell Motil.* 14:311–324. https://doi.org/10.1007/BF00123096

Brynnel, A., Y. Hernandez, B. Kiss, J. Lindqvist, M. Adler, J. Kolb, R. van der Pijl, J. Gohlke, J. Strom, J. Smith, et al. 2018. Downsizing the molecular spring of the giant protein titin reveals that skeletal muscle titin determines passive stiffness and drives longitudinal hypertrophy. *eLife.* 7: e40532. https://doi.org/10.7554/eLife.40532

Eakins, F., C. Knupp, and J.M. Squire. 2019. Monitoring the myosin crossbridge cycle in contracting muscle: steps towards 'Muscle-the Movie'. *J. Muscle Res. Cell Motil.* 40:77–91. https://doi.org/10.1007/s10974-019-09543-9

Harford, J.J., and J.M. Squire. 1997. Time-resolved studies of muscle using synchrotron radiation. *Rep. Prog. Phys.* 60:1723–1787. https://doi.org/10.1088/0034-4885/60/12/005

Haselgrove, J.C. 1975. X-ray evidence for conformational changes in the myosin filaments of vertebrate striated muscle. *J. Mol. Biol.* 92:113–143. https://doi.org/10.1016/0022-2836(75)90094-7

Hudson, L., J.J. Harford, R.C. Denny, and J.M. Squire. 1997. Myosin head configuration in relaxed fish muscle: resting state myosin heads must swing axially by up to 150 A or turn upside down to reach rigor. *J. Mol. Biol.* 273:440–455. https://doi.org/10.1006/jmbi.1997.1321

Huxley, H.E., A.R. Faruqi, M. Kress, J. Bordas, and M.H. Koch. 1982. Time-resolved X-ray diffraction studies of the myosin layer-line reflections during muscle contraction. *J. Mol. Biol.* 158:637–684. https://doi.org/10.1016/0022-2836(82)90253-4

Huxley, H., M. Reconditi, A. Stewart, and T. Irving. 2006. X-ray interference studies of crossbridge action in muscle contraction: evidence from quick releases. *J. Mol. Biol.* 363:743–761. https://doi.org/10.1016/j.jmb.2006.08.075

Knupp, C., G. Offer, K.W. Ranatunga, and J.M. Squire. 2009. Probing muscle myosin motor action: x-ray (m3 and m6) interference measurements report motor domain not lever arm movement. *J. Mol. Biol.* 390:168–181. https://doi.org/10.1016/j.jmb.2009.04.047

Knupp, C., E. Morris, and J.M. Squire. 2019. The Interacting Head Motif Structure Does Not Explain the X-Ray Diffraction Patterns in Relaxed Vertebrate (Bony Fish) Skeletal Muscle and Insect (*Lethocerus*) Flight Muscle. *Biology (Basel).* 8:67. https://doi.org/10.3390/biology8030067

Lange, S., N. Pinotsis, I. Agarkova, and E. Ehler. 2020. The M-band: The underestimated part of the sarcomere. *Biochim. Biophys. Acta Mol. Cell Res.* 1867:118440. https://doi.org/10.1016/j.bbamcr.2019.02.003

Luther, P.K., H. Winkler, K. Taylor, M.E. Zoghbi, R. Craig, R. Padrón, J.M. Squire, and J. Liu. 2011. Direct visualization of myosin-binding protein C bridging myosin and actin filaments in intact muscle. *Proc. Natl. Acad. Sci. USA.* 108:11423–11428. https://doi.org/10.1073/pnas.1103216108

Martin-Fernandez, M.L., J. Bordas, G. Diakun, J. Harries, J. Lowy, G.R. Mant, A. Svensson, and E. Towns-Andrews. 1994. Time-resolved X-ray diffraction studies of myosin head movements in live frog sartorius muscle during isometric and isotonic contractions. *J. Muscle Res. Cell Motil.* 15:319–348. https://doi.org/10.1007/BF00123484

Offer, G., C. Moos, and R. Starr. 1973. A new protein of the thick filaments of vertebrate skeletal myofibrils. Extractions, purification and characterization. *J. Mol. Biol.* 74:653–676. https://doi.org/10.1016/0022-2836(73)90055-7

Piazzesi, G., M. Reconditi, M. Linari, L. Lucii, Y.B. Sun, T. Narayanan, P. Boesecke, V. Lombardi, and M. Irving. 2002. Mechanism of force generation by myosin heads in skeletal muscle. *Nature.* 415:659–662. https://doi.org/10.1038/415659a

Reconditi, M., E. Brunello, L. Fusi, M. Linari, M.F. Martinez, V. Lombardi, M. Irving, and G. Piazzesi. 2014. Sarcomere-length dependence of myosin filament structure in skeletal muscle fibres of the frog. *J. Physiol.* 592: 1119–1137. https://doi.org/10.1113/jphysiol.2013.267849

Rome, E., G. Offer, and F.A. Pepe. 1973. X-ray diffraction of muscle labelled with antibody to C-protein. *Nat. New Biol.* 244:152–154. https://doi.org/10.1038/newbio244152a0

Sjöström, M., and J.M. Squire. 1977. Fine structure of the A-band in cryo-sections. The structure of the A-band of human skeletal muscle fibres from ultra-thin cryo-sections negatively stained. *J. Mol. Biol.* 109:49–68.

Squire, J.M. 1972. General model of myosin filament structure. II. Myosin filaments and cross-bridge interactions in vertebrate striated and insect flight muscles. *J. Mol. Biol.* 72:125–138. https://doi.org/10.1016/0022-2836(72)90074-5

Squire, J.M. 1981. The structural basis of muscular contraction. Plenum Publishing, New York. https://doi.org/10.1007/978-1-4613-3183-4

Squire, J.M. 2000. Fibre and Muscle Diffraction. *In* Structure and Dynamics of Biomolecules. E. Fanchon, E. Geissler, L.-L. Hodeau, J.-R. Regnard, and P. Timmins, editors. Oxford University Press, Oxford, UK. 272–301.

Squire, J. 2019. Special Issue: The Actin-Myosin Interaction in Muscle: Background and Overview. *Int. J. Mol. Sci.* 20:5715. https://doi.org/10.3390/ijms20225715

Squire, J.M., and C. Knupp. 2005. X-ray diffraction studies of muscle and the crossbridge cycle. *Adv. Protein Chem.* 71:195–255. https://doi.org/10.1016/S0065-3233(04)71006-2

Squire, J.M., and C. Knupp. 2017. Studies of Muscle Contraction Using X-ray Diffraction. *In* Muscle Contraction and Cell Motility: Fundamentals and Developments. H. Sugi, editor. Pan Stanford Publishing, Singapore. 35–73.

Squire, J.M., and C. Knupp. 2021. Analysis methods and quality criteria for investigating muscle physiology using X-ray diffraction. *J. Gen. Physiol.* 153:e202012778.

Squire, J.M., P.K. Luther, and C. Knupp. 2003. Structural evidence for the interaction of C-protein (MyBP-C) with actin and sequence identification of a possible actin-binding domain. *J. Mol. Biol.* 331:713–724. https://doi.org/10.1016/s0022-2836(03)00781-2